NASA TECHNICAL MEMORANDUM

NASA TM X-52906

NASA TM X-52906

MEASUREMENT AND ANALYSIS OF LIGHTNING INDUCED VOLTAGES IN AIRCRAFT ELECTRICAL SYSTEMS

by Paul T. Hacker
Lewis Research Center
Cleveland, Ohio

and

J. A. Plumer
General Electric Company
High Voltage Laboratory
Pittsfield, Massachusetts

TECHNICAL PAPER proposed for presentation at 1970 Lightning and Static Electricity Conference sponsored by the Society of Automotive Engineers and the Air Force Avionics Laboratory San Diego, California, December 9-11, 1970

MEASUREMENTS AND ANALYSIS OF LIGHTNING-INDUCED VOLTAGES IN AIRCRAFT ELECTRICAL CIRCUITS

Paul T. Hacker
Aerospace Safety Research and Data Institute
National Aeronautics and Space Administration
Lewis Research Center
Cleveland, Ohio

and

J. A. Plumer
General Electric Company
High Voltage Laboratory
Pittsfield, Massachusetts

E-5991

ABSTRACT

A series of measurements were made of voltages induced in electrical circuits within a metallic aircraft wing by full-scale simulated lightning currents flowing through its skin and structure. The measured data were mathematically analyzed to enable determination of voltages across load impedances to which the circuits might be connected elsewhere in the aircraft. Relationships between induced voltages and lightning current, wing structural and circuit parameters were determined. Induced voltages of magnitudes likely to cause damage or interference with avionics were measured.

LIGHTNING TO AIRCRAFT has been recognized as a hazard for a long time. The hazards to aircraft due to lightning strikes are manifested in several forms, such as:

(1) Damage to the aircraft structure.
  (a) Pitting and holes in metallic surfaces.
  (b) Delamination and loss of strength of composite nonmetallic materials.
(2) Ignite fuels vapors in tanks through
  (a) Holes burned through or hot spots created on the surfaces of integral fuel tank.
  (b) Arcing across electrical discontinuities such as fuel tank filler caps.
  (c) Ignition of vapors at tank vent exits.
(3) Damage to electrical systems and avionic equipment by
  (a) Direct strikes to external electrical components.
  (b) Indirect or induced electrical voltages in electrical systems.

The mechanical effects, items (1a) and (1b), the thermal effects, items (2a), (2b), and (2c), and the direct electrical effects, item (3a), of lightning strikes have been the subject of many investigations conducted by various government agencies, aircraft industries and research laboratories during the past two or three decades. Refs. 1 to 10.

The indirect or induced effects of lightning on aircraft electrical systems have not received much attention. It has been recognized that voltages could be induced in electrical circuits inside the aircraft by lightning currents passing through the aircraft skin and structure. The magnitude of these induced voltages or the extent to which they interact with and affect aircraft electrical and avionic systems has not been determined. Experience has shown that sensitive avionics, as well as other equipment, have been affected by some characteristic of the flight environment when lightning is present. Communication and navigational equipment have failed and electroexplosive devices have also been actuated (1).* The hazards have been lived with for many years and few if any fatal accidents could be attributed to induced electrical effects. In the past, the induced effects were probably not severe enough to cause extensive damage to electronic equipment because such equipment made extensive use of vacuum tubes and large electronic components which inherently have high voltage breakdown characteristics. Modern aircraft avionics, however, make extensive use of semiconductors and micro-circuitry which are much less tolerant to transient overvoltages and currents.

Some investigations have been conducted to establish the transient voltage and current withstand capability of these new electronic devices. These investigations, however, have been mainly concerned with surges in the power supply. Very little effort, however, has been expended to determine the magnitude of induced voltage arising in aircraft electrical circuits due to lightning strikes or the relationship between the induced voltages and the characteristics of the lightning current that produce them. It is necessary to know the magnitude of these induced voltages before the susceptibility of aircraft electrical systems and components to interference or damage

*Numbers in parentheses designate References at end of paper.

can be assessed.

Thus a program was initiated by the Aerospace Safety Research and Data Institute, NASA, Lewis Research Center, to determine the magnitude of induced voltages and currents which may arise in electrical circuitry within a metallic aircraft structure through which lightning current is flowing. The objectives of the experimental and analytical program were to:

(1) Measure the voltages and currents induced in actual aircraft circuits.

(2) Determine the extent to which these voltages may be coupled to any load (equipment) for which the input impedance is known.

(3) Identify and determine the significance of factors affecting these voltages.

(4) Establish and evaluate techniques for eliminating or reducing the magnitude of the induced effects.

(5) Develop techniques which could be used to evaluate the susceptibility of circuits in any aircraft.

The experimental portion of the investigation was performed with a complete wing of an F89J fighter aircraft and a full scale simulated lightning facility. The program was conducted by the High Voltage Laboratory of the General Electric Company in Pittsfield, Massachusetts. This paper outlines the investigation and presents some of the significant results. Details of the investigation are presented in a General Electric report, HVL 69-161 (11).

THEORETICAL ANALYSIS

INDUCED VOLTAGE MECHANISMS - Voltages can be induced in electrical circuits inside aircraft structures by lightning currents flowing through the structure by:

(1) Magnetic coupling between the current carrying structure and other circuits.

(2) Resistive voltage rises in the structure to which electrical conductors or shields may be connected.

Figure 1 is an electrical circuit representation of an aircraft wing-electrical circuit combination which illustrates how induced voltages are generated. Lightning current, i_L, flowing in the skin and structure generates a magnetic field which links the electrical circuit. This magnetic coupling is indicated by the lumped inductances, L_W and, L, for the structure and circuit respectively. These two inductances possess a mutual inductance, M. Most of the magnetic flux, φ_o, generated will be outside the wing, but a significant amount, φ_i, will be generated inside the wing because of the non-cylindrical geometry and the finite conductivity of the wing. The flux distribution is further complicated by the location of internal structural members, rivetting, skin joints, access openings and openings created by flight control surfaces. The lightning current flowing through the structure also produces a voltage rise along the wing due to the finite resistance, R_W, of the wing. This voltage rise appears in the electrical circuit. In addition to the electrical resistance of the structural material, other sources of resistance are the bondings resistances which appear at junctions; between skin sections, between skin and structural members, or between structural members. The magnetic coupling and resistive voltage rise produce a voltage, e_{oc}, between terminals a and b.

The circuit of Fig. 1 is illustrated in more conventional form in Fig. 2. The open circuit voltage, e_{oc}, appearing across terminals a and b is composed of the magnetically induced voltage, V_M, and the resistive voltage rise, V_R. The magnetically induced voltage is equal to the rate of change of flux coupling the circuit, that is

$$V_M = d\varphi_i/dt \tag{1}$$

The rate-of-change of flux is equal to the product of the mutual inductance, M, and the rate-of-change of current, that is

$$(d\varphi_i/dt) = M(di_L/dt) \tag{2}$$

Thus the magnetically induced voltage is given by

$$V_M = M(di_L/dt) \tag{3}$$

The resistive voltage rise, V_{R_W}, is given by the product of the current and the resistance of the structure along the current path, that is

$$V_{R_W} = i_L R_W \tag{4}$$

The total open circuit induced voltage, e_{oc}, at terminals a and b is the sum of Eqs. (3) and (4).

$$e_{oc} = M(di_L/dt) + i_L R_W \tag{5}$$

The total induced voltage is a function of the rate of change and the absolute value of the lightning current flowing in the wing. Measured characteristics of lightning (12), (13) show that rates of current change of 15 kiloamperes per microsecond and peak current values of 30 kiloamperes are very common. These are fairly large values and would result in large induced voltages if the mutual inductance, M, and the effective resistance, R_W, are significant. The rate-of-change of the magnetic flux linking the circuits or the mutual inductance, M, cannot be readily calculated. The effective wing resistance, R_W, is not the simple direct current resistance of the structure. It is a complex time-varying function of the wing geometry, conductivity and thickness and the time characteristics of the lightning current.

These two factors are thus best determined experimentally. The method used to determine the effective wing resistance and mutual inductance from experimental data by the use of Eq. (5) is presented in the REDUCTION OF DATA SECTION.

The circuit depicted in Figs. 1 and 2 utilized the aircraft structure as a return path. There are circuits present in aircraft which are open ended or "floating" such as antenna and circuits which utilize a separate ground return. In these circuits, the resistive induced voltages will not directly appear across the circuit terminals. There may be, however, an induced voltage due to capacitive coupling between the current carrying structure and the "floating" electrical circuit.

THEVENIN EQUIVALENT CIRCUITS - In the experimental tests of simulated lightning strokes to a full scale F89 wing, which will be described later, the open circuit induced voltages were measured for several circuits at the root end of the wing. The open circuit voltage has little practical significance by itself. What is of importance is the voltage induced across an impedance load (aircraft electrical equipment) to which the circuit is connected, since this voltage determines whether or not damage will occur. The voltage induced across any load in the aircraft to which the wing circuit might be connected can be predicted by determining the Thevenin equivalent circuit for each wing circuit. The Thevenin Equivalent Circuit for the wing electrical circuit of Fig. 2 is illustrated in Fig. 3. The Thevenin Equivalent Circuit consists of a voltage source, e_T, in series with an impedance, Z_T, between the terminals a and b. Comparing the circuits of Figs. 2 and 3, the Thevenin voltage source, e_T, is equivalent to the open circuit voltage, e_{oc}, developed by the mutual inductance and resistive voltage rise across resistance, R_w. Since the open circuit voltage is a function of the lightning current, i_L, Eq. (5), then the Thevenin voltage is also a function of the lightning current or

$$e_T = R_w i_L + M(di_L/dt) \tag{6}$$

By definition the Thevenin impedance, Z_T, is given by

$$Z_T = e_T/i_{sc} \tag{7}$$

where i_{sc} is the current flowing in the circuit when the terminals a and b are shorted.

If a load of impedance, Z, is connected across terminals a and b of Fig. 3, the voltage drop across the impedance, V_Z, is given by

$$V_Z = Z/(Z_T + Z)e_T = Z/(Z_T + Z)e_{oc} \tag{8}$$

Combining Eqs. (7) and (8) gives

$$V_Z = (Zi_{sc}e_{oc})/(Zi_{sc} + e_{oc}) \tag{9}$$

which indicates that the voltage developed across any impedance, Z, attached to the terminals of the circuit is a function of the open-circuit voltage and the short-circuit current developed in the wing circuit. Thus, in the experimental program both the open-circuit voltage and short-circuit current were measured and recorded oscillographically as a function of time. To use these measured values of open-circuit voltage and short-circuit current in the solution of Eqs. (7), (8), and (9), they have to be transformed into the complex frequency domain since Eqs. (7), (8), and (9) apply in this domain.

The Thevenin impedance, Z_T, may be assumed composed of a combination of resistances and reactances, such as the series connected resistance, R, and inductance, L, shown in Fig. 3. To understand and possibly predict the induced voltage response of a circuit, a knowledge of the magnitude of the components of the circuit impedance is required. A method by which values of effective circuit resistance and inductances can be calculated from measurements of open-circuit voltages and short-circuit currents is presented in the REDUCTION OF DATA SECTION.

EXPERIMENTAL INVESTIGATION

The experimental investigation was performed using a complete right wing of an F89 aircraft and a full scale simulated lightning test facility.

DESCRIPTION OF WING -

Physical Characteristics - A schematic of a plan view of the wing showing approximate size and main components is given in Fig. 4. The wing is of full cantilever, multispar construction using heavy, tapered alclad skin. The principal components are the main wing panel, leading edge, trailing edge and a non-jettisonable wing tip pod.

The main wing panel consists of five heavily constructed spanwise spars, bulkheads, ribs and aluminum honeycomb reinforced heavy tapered alclad skin. The main panel houses a retractable main landing gear and six fuel cells. Access and inspection doors are provided throughout the wing surface.

The leading edge consists of spars, formed ribs, heavy tapered alclad skin and a spanwise anti-icing hot air duct. The leading edge is attached to the forward wing spar with flush-headed screws.

The trailing edge section is divided into a slotted wing flap on the inboard portion and a combination aileron speed brake on the outboard portion. The attachments and actuating devices for these aerodynamics control surfaces required fairly large opening into the interior of the main wing section which could allow externally generated magnetic flux to enter.

The wing is equipped with a 600 gallon wing tip

fuel tank. The tank is mounted on the wing by two bolts and a pin. Flexible fuel hose and electrical cables provide necessary connections between the wing and tip tank.

In general, the alclad wing skin increased in thickness from the wing tip to root. In the main wing panel, the skin thickness ranged from 0.154 to 0.291 in. In the leading edge section, the skin thickness ranged from 0.085 to 0.157 in. In the trailing edge, aerodynamic control surfaces the alclad thickness range from 0.051 to 0.072 in. The thicknesses were required for the mission of the F89 aircraft and are much thicker than some of those found in recent commercial or military aircraft. As a result, the electromagnetic shielding effectiveness of this wing is likely to be greater than that of a wing covered with thinner skins.

The exterior surfaces of the wing skins were chromodized with aladine 1000. The interior wing skins and structural elements were treated with Iridite 14-2, chromic acid anodized and then covered with a green zinc chromate primer. This treatment was given all surfaces, including the mating surfaces between elements. No treatment for improvement of electrical bonding between surfaces was applied. Thus, the resultant electrical bonding between structural elements is mainly accomplished by the fastening rivets and bolts.

Wing Electrical Circuits - The wing contained 29 functional electrical circuits for such functions as: aircraft position light, fuel quantity gages, fuel booster pumps, fuel vent valves, glide slope antenna, and several safety and indicating switches on movable components in the wing. The number of conductors in each circuit ranges from one to more than twenty. There were a large variety of circuits in regards to the type of return path and type of shielding employed. For the investigation only eight circuits were studied. The criteria used for the selection of these eight circuits included:

(1) Function of the circuit.
(2) Location of the circuit.
(3) Type of return path.
(4) Shielding employed.
(5) Applicability to other aircraft.
(6) Characteristics of the circuit.

For this paper, however, only the results for some of the circuits will be presented and discussed. The description of the other circuits along with results of tests are presented in (11). In addition to the regular aircraft circuit, a special multiconductor circuit was installed in the wing to make comparative tests on various types of shielding and length and location of circuit. Results for this circuit will also be presented. A description of each circuit discussed herein is given in the RESULTS AND DISCUSSION SECTION when the test results are presented.

TEST SETUP - The wing was supported on a portable wooden carriage which was positioned adjacent to a high-amplitude simulated lightning current generator in an indoor test bay of the G. E. High Voltage Laboratory. The test setup is shown schematically in Fig. 5. The simulated lightning strike was delivered to the desired location on the wing by the use of a movable electrode. The arc gap from electrode to wing was approximately 8 in. The root end of the wing was joined to a double walled screened instrument enclosure into which the simulated lightning currents passed from the wing. The lightning current return flow path from instrument enclosure to the impulse generator was through a low-inductive aluminum foil along the floor. A current measuring shunt was located in the lightning current circuit at the junction of the instrument enclosure and aluminum foil. A photograph of the wing in the test area is shown in Fig. 6.

TEST CONDITIONS -

Lightning Simulation - The currents which pass through an aircraft when it is struck in flight by natural lightning are believed to be a combination (2, 3) of high-amplitude, short duration "strokes" and low-amplitude, long duration approximately constant value "continuing currents." This combination may be repeated several times in a lightning discharge.

The continuing currents are known to produce thermal and mechanical damage to aircraft skins (3, 4). These currents, however, create very little magnetic flux, and that which is created does not change rapidly. As shown by Eq. (5) in THEORETICAL ANALYSIS, a rapidly changing current or magnetic flux is required to induce voltages in magnetically coupled circuits. Therefore, only the high-amplitude, short-duration strokes were simulated for all of the tests in this program. The current strokes generated were critically damped to obtain a unidirectional wave shape, since natural lightning currents are nearly always unidirectional. Since natural lightning strokes may vary in wave shape, amplitude, polarity and attachment location, it was desirable to evaluate the effects of each of these variables upon the voltages induced in internal circuits.

Two wave shapes were used for most of the test. These shapes are designated as "fast" and "slow." The meaning of these terms and a standard wave shape notation is illustrated in Fig. 7. An impulse current, simulating a high-amplitude, short duration lightning stroke is ideally an aperiodic transient current which rises rapidly to a maximum value and falls less rapidly to zero. The standard notation is based upon the time to crest, T_1, and the time to 50% value, T_2, on the decay. The wave shape is then described by the notation: $(T_1 \times T_2)$. In this notation, the two wave shapes used in most of the tests are $(36 \times 82\ \mu s)$ and $(8.2 \times 14\ \mu s)$ for the "slow" and

"fast" respectively. Oscillograms of these current wave shapes are shown in Fig. 8. For these oscillograms and others presented later, the size of the ordinate and abscissa divisions are shown on the bottom left and bottom right respectively.

To identify those stroke locations creating the most severe induced voltages, a series of preliminary strokes were applied to each of ten locations shown on Fig. 9. An identical 14 kiloampere (12×24 μs) simulated lightning discharge was applied to each location. Open-circuit voltages and short circuit currents were measured at the wing root terminals of two circuits. One circuit was located in the trailing edge and extended the full length of the wing. The other was in the leading edge and extended to about half span. The five position indicated by the large circles in Fig. 9 gave the largest induced effects and were, therefore, used through the remainder of the tests.

It was postulated before any tests were performed, that the induced effects for a given wave shape might be a linear function of the current stroke amplitude. A series of tests early in the experimental program using a (12×24 μs) wave shape and stroke amplitudes from 7 to 70 kiloampere showed a near linear relationship. Thus to minimize the number of tests to be performed most of the remaining tests were made at a stroke amplitude of 40 kiloamperes. This value is near the average amplitude of measured lightning strikes (14). At a maximum current amplitude of 40 kiloamperes the "fast" wave shape (8.2×14 μs) provides an initial rate of change of current (di_L/dt) of 8 kiloamperes per microsecond which is four times as fast as that for the "slow" (36×82 μs) stroke (2KA/μs).

MEASUREMENTS - Measurements made at the wing root end of each circuit for each applied simulated lightning stroke condition included:

(1) Open-circuit voltage, e_{oc}.

(2) Short-circuit current, i_{sc}.

(3) Voltage across a terminating dummy load, e_l.

(4) Current through a terminating dummy load, i_l.

The induced effects were measured for the dummy load to provide a check on the calculated response to the same load impedance using the Thevenin Equivalent Circuit determined from the open and closed circuit tests. The dummy load was a 1 ohm resistance. Measurements were recorded oscillographically using a Tektronix Type 535 oscilloscope with a Type 1A1 preamplifier. Measurements were made at one or more oscilloscope sweep settings as necessary to define the wave shape of the signals being measured. Typical oscillograms of open-circuit voltages and short-circuit currents are shown in Fig. 10. As might be expected from the pulse nature of the applied simulated lightning current and the dependency of the induced open-circuit voltage on the rate of change of the lightning current, Eq. (5), the open-circuit voltage and short-circuit current are both time dependent. They reach a maximum value on the first half cycle and decay rapidly.

For many of the circuits and test conditions, there was a very high frequency damped oscillation at the beginning of the open-circuit voltage trace. This oscillation was not always visible on the oscillograms due to smearing unless fast sweep was used. The amplitude of the first cycle of this high frequency was usually much larger than the amplitude of the slow wave shown in Fig. 10. The amplitude and wave shape of the applied lightning current were monitored and recorded oscillographically for all tests to assure that the desired wave shape was being applied.

The measuring instruments were located inside the double-screened shielded enclosure attached to the root end of the wing. This enclosure provided a magnetic shielding of the oscilloscopes and measurement leads, into which extraneous voltages could otherwise be induced by the strong magnetic field generated by the simulated lightning stroke itself. Checkout tests with the measuring equipment plus measurement of magnetic flux inside the enclosure indicated that the instrument system was not being influenced.

In circuits employing only a single conductor, in which the airframe or a coaxial shield is used as the return path, measurements were always made between the conductor and the airframe or shield. Some circuits, however, have more than one conductor and some do not employ the airframe as a return path. In these cases, measurements of induced voltages and currents were made between pairs of conductors and between individual conductors and airframe when the airframe was used as part of the circuit.

REDUCTION OF DATA

The basic data recorded during the investigation were the open-circuit voltage and short-circuit current for the various circuits, lightning current wave shape and stroke location. These data were reduced and analyzed to determine the following:

(1) Maximum values of induced open-circuit voltages and short-circuit currents.

(2) Values of effective wing resistance and mutual inductance.

(3) Values of effective circuit resistances and inductance.

The maximum values of induced open-circuit voltage and short-circuit current were obtained directly from the respective oscillograms. The other parameters were derived by calculation.

EFFECTIVE WING RESISTANCE, R_W, AND MUTUAL INDUCTANCE, M - The effective wing resistance, R_W, and the mutual inductance, M,

between the wing structure and the electrical circuits were obtained through the use of Eq. (5).

$$e_{oc} = R_w i_L + M(di_L/dt) \quad (5)$$

If it is assumed that the effective wing resistance, R_w, and the mutual inductance, M, are not a function of time or lightning current, then they can be evaluated directly from the oscillogram traces for the open-circuit voltage, e_{oc}, and the lightning current, i_L. The calculation can be illustrated by the use of Fig. 11 which shows a typical lightning current and corresponding induced open-circuit voltage wave form. At time, T_1, the rate of change of lightning current with time, (di_L/dt), equals zero. Equation (5) then becomes

$$e_{oc_1} = R_w i_{L_1}$$

or

$$R_w = e_{oc_1}/i_{L_1} \quad (10)$$

where values of e_{oc_1} and i_{L_1} can be obtained from the respective curves at time, T_1. At time, T_2, the induced voltage is zero and Eq. (5) reduces to

$$M(di_L/dt)_2 = -R_w i_{L_2}$$

or

$$M = -R_w i_{L_2}/(di_L/dt)_2 \quad (11)$$

The value of the mutual inductance, M, can then be calculated by Eq. (11) by obtaining values of i_L and $(di_L/dt)_2$ from the lightning current trace at time T_2 and the value of the effective wing resistance calculated above by Eq. (10). The above equations illustrate how the effective wing resistances and mutual inductances could be calculated by hand. In the investigation, however, these equations were solved by a computer using approximately mathematical expressions for both the lightning current and the open-circuit voltages as inputs to the computer.

EFFECTIVE CIRCUIT RESISTANCE, R, AND INDUCTANCE, L - The Thevenin impedance, Z_T, as given by Eq. (7) is resolved into an effective resistance, R, and an effective inductance, L, for a wing electrical circuit by the following technique. Using the oscillograms of open-circuit voltage and short-circuit current obtained for a given circuit and test condition, approximately analytical expressions are written for both as a function of time. These analytical expressions are then transformed into the complex frequency domain by the use of the Laplace Transform. After the transformation, the ratio of the open-circuit voltage to short circuit current is calculated as required by Eq. (7). The real part of the resulting complex expression is the resistive portion of the impedance and the imaginary part is the inductive portion.

RESULTS AND DISCUSSION

Typical experimental data and analytical results obtained during the investigation on: (1) induced voltages and currents, (2) effective wing resistance and mutual inductance, and (3) effective circuit resistance and inductance as functions of lightning current amplitude, wave shape and stroke location are presented in Figs. 13, 14, 15, 16, and 19 and Tables I through VII and discussed in the following section. Most of the data presented are for the position light, the E-11 autopilot and the specially installed circuits. Figures 12, 17, and 18 show the location and schematic diagram of these circuits.

CIRCUIT L.050, POSITION LIGHT - The location of this circuit within the wing and wiring schematic is shown in Fig. 12. (Note: On this figure and other places throughout the report, the USAF Code numbers for circuits, conductors, and connectors in the F89J are indicated.) The circuit is routed along the trailing edge of the main span, and is partially exposed in the area of the flap. The circuit passes through the tip fuel tank to the position light. In the fuel tank the circuit is enclosed in a conduit. The airframe is used as a return path. The bulb has a resistance of 2.5 ohms. Perhaps because this circuit extends the longest, is partially exposed, and employs the airframe as a return path, the induced voltage and currents measured were the greatest found in any of the circuits tested. As a result of this, and because this circuit is representative of a type found commonly in many aircraft, the position light circuit was more extensively studied than the others.

Induced Effects - The induced open-circuit voltages and short-circuit currents were measured for various stroke amplitudes, locations, and wave shapes. A preliminary series of tests using a moderately fast (12×24 μs) simulated lightning stroke were made to determine the relationship between the induced effects and the lightning current amplitude. The maximum current amplitude was varied from 7 to 90 kiloamperes. Figure 13 shows the results of these tests. The data points represent the maximum values measured. Both the open-circuit voltage and short-circuit current show an almost linear variation with current amplitude. Based upon these results, most of the subsequent tests were performed at 40 kiloamperes.

Figures 14 and 15 show a complete set of oscillograms for open-circuit voltages and short-circuit currents for five different stroke locations and for both the "slow" (36×82 μs) and "fast" (8.2×14 μs) wave shapes respectively. For the "slow" wave shape the induced voltages ranged between 2 and 20 volts and the induced currents ranged between 0.7 to 9.0 amperes. For the "fast" wave

shape the voltages and currents were greater by about a factor of two in most cases than for the corresponding "slow" wave shape cases. Variations in stroke location resulted in significant changes in induced voltages and currents. In general, delivery of strokes to locations farthest out on the wing and closest to the location of the circuit resulted in the highest voltages. All of the voltage wave shapes shown in Figs. 14 and 15 are composed of both a resistive voltage, in phase with the applied lightning current wave form, and a magnetically induced voltage, proportional to the rate of change of the applied lightning current. The inductive component, as evidenced by high initial rise rate and an undershoot, is greater for the stroke locations closest to the circuit (locations 1 and 5) than for the locations farther away. In the more distant stroke locations, the resistive component seems to be predominant. The voltages induced across and the current through a 1 ohm load resistor placed across the circuit terminals at the wing root end were also measured for the two current wave shapes and 5 stroke locations. The maximum voltage and currents measured are tabulated in Table I along with the corresponding maximum open-circuit voltages and short-circuit currents. As would be expected, the load resistor decreased the induced voltages and currents. In the table, two values of voltages are given for many of the cases. The first value listed is the maximum value of the first half cycle of the high frequency component that occurred in many cases at the beginning of the induced wave. The second value listed is the maximum induced in the slower component of the induced wave.

Wing Resistances and Mutual Inductances - The effective wing resistance, R_W, and mutual inductance, M, were calculated for the position light circuit using the method outlined in the REDUCTION OF DATA SECTION. These calculated values are tabulated in Table II for the two lightning current wave shapes and the five different stroke locations. The data indicate that both the effective wing resistance and mutual inductance are a function of both the applied wave shape and the location of the stroke. As would be expected from the induced effects described above, the largest values of effective wing resistance and mutual inductance occurred for strokes delivered to the wing tip tank. Although the applied wave shapes gave different results, there does not appear to be any consistent trend. For two cases with the "fast" wave shape, negative values of effective resistance were calculated. Negative values of mutual inductances were encountered with other circuits tested. Since a negative element is not possible, the negative values must be due to some other anomaly. Possibly they are the result of the lightning current flowing in a direction with respect to the wing circuit path opposite from that assumed for derivation of the equation which was used as a basis for the calculation. It should be realized that the resistance and mutual inductances calculated are effective values and as such do not describe tangible wing characteristics.

In the derivation of the method for calculating the effective wing resistance and mutual inductance, it was assumed that these two parameters did not vary with time. To verify this assumption, values of effective resistance and mutual inductance were calculated. The values were then used in the Thevenin Equivalent Circuit Equation (Eq. (5)) along with the applied lightning current to calculate the open circuit voltage as a function of time. The results of this calculation are shown in Fig. 16. The agreement with measured induced voltages is very good for the first half cycle.

Circuit Impedances - The effective circuit resistance, R, and inductances, L, were calculated for the position light circuit using the method outlined in REDUCTION OF DATA SECTION. These calculated values are tabulated in Table III. These data show that there is some variation in circuit impedances as a function of stroke location and wave shape. The variations, however, are not as great as was the variation in calculated values of effective wing resistance and mutual inductance for the same test conditions. The values of resistance calculated, 1.23 to 3.09 ohms, compare favorably with the resistance of the light bulb which was 2.5 ohms. The values of inductance calculated for this circuit appear reasonable for a conductor of its length. It appears from all the data obtained in the program that the effective impedances closely approximate the actual wing circuit impedances. A negative inductance was obtained for one test condition.

CIRCUIT F.0511, E-11 AUTOPILOT - The location of this circuit within the wing and a wiring schematic is shown in Fig. 17. This circuit is a part of the autopilot. It extends along the trailing edge to a safety switch located adjacent to the leading edge of the aileron. Its function is to assure that the aileron is in neutral position before firing of rockets which are carried on a pylon below the wing. Both connectors of the circuit are isolated from ground. The circuit is not shielded and is exposed to the outside of the wing for a short distance when the aileron is deflected. The circuit was tested with the safety switch in the closed position and the data presented below were obtained across the two conductors of the circuit.

Induced Effects - The open-circuit voltages, short-circuit currents, the voltages across and current through a 1 ohm load resistor for the same test conditions used on the position light circuit are presented in Table IV. The induced effects are much less than for the position light circuit. The maximum open-circuit voltage (slow component of

wave) was 0.6 volt which was produced by the "fast" lightning wave shape to stroke location number 5. Stroke location number 5 is the closest to the circuit. The short-circuit currents measured were 0.5 amperes or less. The 1-ohm load resistor decreased both the voltages and currents measured but not markedly. The position light circuit is longer than this circuit and in addition, this circuit does not employ the airframe as part of the circuit. The variation of the induced effects due to stroke location and lightning current wave shape is not as great as with the position light circuit.

Wing Resistance and Mutual Inductance - Equation (5), by which the effective wing resistance, R_W, and mutual inductance, M, were calculated for the position light circuit above, was derived on the basis of circuits which use the aircraft structure as part of the electrical circuit. This Autopilot circuit does not use the structure as part of the circuit. Nevertheless, it was found possible to calculate values of effective wing resistance and mutual inductance for circuits which are "floating" or not terminated either directly or indirectly to the aircraft structure.

The calculated effective wing resistance and mutual inductance for the Autopilot circuit are presented in Table V. The largest effective wing resistance was 10.0 microhms for a "fast" wave shape at stroke location number 7. The largest absolute value of effective mutual inductance was 0.187 nanohenry, again for the "fast" wave shape but at stroke location number 4. The calculations show that these parameters for this circuit are also a function of stroke position and applied current wave shape. The values are much less than those for the position light circuit for the same conditions. For this circuit all the mutual inductances were negative.

For "floating" circuits, capacitive coupling between the circuit and the current carrying structure may contribute to the induced voltage. The magnitude would be small compared to that induced magnetically or due to resistive voltage rises.

SPECIAL CIRCUITS - Several additional circuits were assembled and installed in the wing for the purpose of making some comparative measurements, which could not be made satisfactorily with circuits already existing in the wing. The measurements desired were:

(1) Comparison of voltages induced in circuits of different length which lead to the same location.

(2) Comparison of voltages induced in a parallel pair and a twisted pair of conductors.

(3) Comparison of voltages induced in a single unshielded conductor and a coaxial cable.

For these tests, a group of conductors suitable for the above comparisons was assembled and installed in the wing as shown in Fig. 18. The conductors were passed from the instrument enclosure through the leading edge heating duct to the wing tip, thence between the wing tip and tip fuel tank and along the outside of the trailing edge spar to the instrument enclosure. Both ends of each conductor were thus terminated in the enclosure.

The circuits include a conductor bundle containing a single insulated number 16 conductor, a single coaxial cable (RG 58A/U), a twisted pair of number 16 insulated conductors, and a parallel pair of number 16 insulated conductors. In order that the circuits would not be completely exposed anywhere along the path, part of the bundle was shielded by copper braid. This braid was placed over the conductor bundle for its entire path except where the bundle was within the heating duct. The copper braid did not cover the bundle within the heating duct because the duct itself provided shielding for the conductors within it. The braid was solidly connected to the airframe at the point where the bundle leaves the heating duct, and at various points along the trailing edge.

All measurements on these circuits were made with 40-kiloampere "fast" (8.2×14 μs) simulated lightning strokes delivered to location 1 at the forward end of the tip fuel tank.

Two series of measurements were made. The first series consisted of measurements of the voltages induced in the entire length of each conductor. These measurements were obtained by measuring the voltages at each end of each conductor, with the other end connected to the airframe. For the second series of measurements, all conductors, including the coaxial cable shield and the copper braid, were solidly connected to the airframe at a point in the trailing edge between the aileron and flap positions, shown on Fig. 18. This in effect created two sets of circuits terminating at the same point in the wing, but following different paths. The circuits passing through the heating duct and across the wing tip were the longest, at 38 feet. Those running out the trailing edge were only 12 feet long. Identical tests and measurements were made in each set of circuits. Measurements were made from all conductors to the airframe (line to airframe), and between each conductor of the twisted and parallel pairs. The open-circuit induced voltages and short-circuit currents measured in each conductor are listed in Tables VI and VII. The maximum amount of voltage measured in any circuit was 6 volts. This relatively low value is probably due to the overall shielding provided all of the circuits. Placement of these circuits in the leading edge heating duct afforded them greater shielding than they would have if simply routed through the leading edge itself. Similarly, the addition of the copper braid around the rest of the circuit provided greater shielding than was afforded the existing aircraft circuits which followed the same path.

Comparison of voltages induced in the various circuits is of interest. When measured between individual conductors and the airframe, it was found that voltages induced in conductors of the parallel pair were three to six times greater than those induced in the twisted pair (Table VI and VII). Voltages measured between conductors of the parallel pair were between two and ten times greater than those measured in the twisted pair.

A comparison between conductor to airframe voltages measured from the individual number 16 insulated conductor and the center conductor of the RG 58A/U coaxial cable shows little difference in voltage amplitudes (Tables VI and VII). This is probably the result of the substantial attenuation in induced voltages provided both of these circuits by the heating duct and copper braid covering all circuits.

An additional interesting comparison is between the long (leading edge) circuits and the short (trailing edge) circuits, both of which terminate at the same point in the wing. Open-circuit voltages and short-circuit currents measured in the longer circuits were greater in all cases than those associated with the shorter ones. Such a result would be expected, since induced effects are believed to be proportional to circuit length (among other factors).

Similar comparisons were found for short-circuit currents, although the comparison ratios for currents were not the same as corresponding voltage ratios. This would be expected for, while voltages are somewhat proportional to circuit length, currents would be proportional to voltages only to the extent they are not diminished by the additional circuit impedance provided by longer circuits.

These measurements illustrated some important facts, the most significant of which are that a twisted pair of conductors receives substantially less induced voltage than a parallel pair, and that circuits within a shielding braid or conduit are much less susceptible to induced voltages than those relying upon the wing skin itself for shielding.

VOLTAGES ACROSS CIRCUIT LOAD IMPEDANCE - One of the objectives of the investigation was to develop a technique by which the voltage induced across any load impedance attached to the wing root end of a circuit could be predicted from the open-circuit voltage and short-circuit current measured at the same point. Towards this end, a technique, expressed by Eq. (9), was derived based on the Thevenin Equivalent Circuit (see THEORETICAL ANALYSIS). To check the validity of the method, the voltage drop across a 1-ohm resistive load as a function of time was calculated from open-circuit voltage and short-circuit current measurements and compared to actual measurements of voltages developed across a 1-ohm resistor. A sample comparison is shown in Fig. 19. The wave shape and especially the maximum voltage developed show fair agreement indicating that the Thevenin Equivalent Circuit may be useful in determining the approximate level of lightning induced voltages which a wing circuit would impress upon various load impedances.

MISCELLANEOUS RESULTS - Two other observations made during the investigation are worthy of mention. First, a reversal of polarity of lightning current did not produce any significant changes in the induced effects. Second, a radio frequency interference filter was employed in a motor circuit (fuel booster pump). The induced open-circuit voltage wave form was similar to those measured for other circuits but the short-circuit current measurements showed a high-frequency damped oscillation which lasted about five times longer than the open-circuit oscillation. This illustrates the possibility that the addition of a device to an electrical circuit to provide protection against one type of electrical phenomenon may aggravate the lightning induced voltage problem.

CONCLUDING REMARKS

The investigation has shown that lightning strikes to aircraft can induce voltages in electrical circuits inside the metal structure through magnetic coupling and voltage rises in the airframe. The magnitude of the induced voltages is a function of the rate of rise of the lightning current, the amplitude of the lightning current, the location of the lightning stroke with respect to the circuit location, and the physical and electrical characteristics of the electrical circuit. The maximum induced voltage measured in any circuit was 96 volts which was produced by a 40 kiloampere discharge with a rate of current rise of 8 kiloamperes per microsecond. Most of the tests were conducted with current rates of rise between 2 and 8 kiloamperes per microsecond and at a current amplitude of 40 kiloamperes. In natural lightning, 20% of all strokes exceeds a peak amplitude of 70 kiloamperes and rates of current rise of 20 kiloamperes per microsecond. To cover the probable range of natural lightning military specification MIL-B-5087B for electrical bonding and lightning protection testing for aerospace systems requires a peak amplitude of 200 kiloamperes and a current rate of rise of 100 kiloamperes per microsecond. Exposure of the F89 wing to either natural lightning or the military specification could induce voltages in the circuits much greater than those measured in the investigation.

A part of the induced voltage in circuits that utilizes the structure as a return path is due to a resistive voltage rise in the structure due to the flow of the lightning current. This voltage rise

depends upon the electrical conductivity of the structural material and the length of the current path. The F89 wing is relatively short and has relatively thick wing skins compared to modern transport aircraft. The wing material is aluminum which has a low electrical resistivity compared to the metals used or proposed for use on modern aircraft. The modern large aircraft may therefore be susceptible to much higher induced voltages than was found in this investigation. The induced voltage problem may be accentuated by the use of nonmetallic, high electrical resistance materials.

Considerable variation was evident in voltages induced in the various circuits tested. An identical stroke could induce up to 96 volts in some circuits, while only a few millivolts in others. The characteristics of the circuits which received the greatest and the least induced voltages are therefore of interest. In general, these characteristics can be summarized as follows:

Circuit characteristics	Circuit return path	Circuit termination (within wing)	Shielding	Routing	Length
Highest voltages	Use airframe as return	Through low impedance component to airframe	Unshielded and exposed to outside of wing	Exposed to outside and routed across joints to mechanically attached assemblies	Extending through full
Lowest voltages	Use separate conductor as return	Through high impedance element to separate return conductor	Shielded and completely enclosed by wing	Unexposed and entirely within wing enclosure	Extending only short distances in wing

From the above summary, it is apparent that the level of lightning induced voltages is considerably dependent upon the characteristics of the individual circuits. As a result, rearrangement or modification in aircraft electrical circuits where possible in the light of the above findings may be an effective means of minimizing the effects of lightning on aircraft electrical systems.

The method of analysis of data utilized in this program has proven to be effective as a means of determining the amount of open-circuit induced voltage actually impressed upon a load impedance to which the circuit is connected, provided reliable open-circuit and short-circuit measurements can be made. Of equal or greater significance, however, is the ability to analytically relate, in nearly all cases, the measured induced voltages to the lightning current wave shape and amplitude, as well as some effective wing parameters. While the effective wing parameters of resistance and mutual inductance have yet to be expressed in terms of tangible wing characteristics, they do shed light upon the qualitative effects of these electrical characteristics of the wing. These relationships enable greater understanding of the factors permitting lightning to induce significant voltages in aircraft electrical circuits.

One objective mentioned in the INTRODUCTION which has not been discussed is the development of techniques which could be used to evaluate the susceptibility of circuits in any aircraft. The analytical techniques developed during the investigation have significance towards this objective but of greater interest was a preliminary series of tests in which a transient analyzer was used to provide low-amplitude nondestructive current surges to the wing. The transient analyzer is a device developed by the High Voltage Laboratory for similar transient response studies of large power transformers. In this series of tests, the induced voltage response to low-level currents from the transient analyzer was compared with similar measurements of voltages induced by full-acale lightning currents. The comparison was favorable, indicating that the results of low-level tests can be scaled proportionately upward to determine the results obtainable from full-scale lightning currents.

These tests indicated that the transient analyzer has validity as a method of determining induced voltage levels in aircraft circuits. In fact, it has several advantages over the full-scale technique. Aside from being physically portable, it has an electrical versatility lacked by most full-scale impulse generators, and can generate a much wider range of wave shapes. For example, it can generate currents with rise times many times faster than those obtainable with a full-scale impulse generator. This will enable evaluation of induced voltages resulting from a much wider range of lightning current wave shapes than possible with full-scale tests. This practical and nondestructive technique may be applicable to the determination of possible induced voltages in the circuits of operational aircraft. In such a case, the

actual voltages and currents associated with the normal aircraft equipment would be measurable, since this equipment would, of course, already be connected to the circuits.

REFERENCES

1. G. E. Morgan, "Investigation of Inadvertent Firing of Electroexplosive Subsystems on Aerospace Vehicles." Interim Technical Report, AF-33(615)-3853, North American Aviation Inc., August 1966.

2. B. J. Peterson and A. R. Wood, "Measurements of Lightning Strikes to Aircraft." Final Report No. DS-68-1 Federal Aviation Administration, January 1968.

3. J. H. Hagenguth, "Lightning Stroke Damage to Aircraft." AIEE Trans., Vol. 68, Part II, pp. 1036-1044, 1949.

4. F. L. Kester, M. Gerstein, and J. A. Plumer, "A Study of Aircraft Fire Hazards Related to Natural Electrical Phenomena." NASA Publication No. CR-1076, 1967.

5. M. J. Kofoid, "Lightning Discharge Heating of Titanium Aircraft Skins." Boeing Scientific Research Laboratories Document, D1-82-0752, September 1968.

6. J. D. Robb, E. L. Hill, M. M. Newman, and J. R. Stahmann, "Lightning Hazards to Aircraft Fuel Tanks." NACA TN 4326, September 1958.

7. J. D. Robb, J. R. Stahmann, and L. A. Hoehland, "Lightning Electrical Hazards to Flight Vehicles." Lightning and Transients Research Institute, AFAL-TR-69-269, December 1969.

8. M. M. Newmann, J. D. Robb, and J. R. Stahmann, "Lightning Protection Measures for Aircraft Fuel Systems, Phase I." Lightning and Transients Research Institute, FAA Technical Report ADS-17, May 1964.

9. M. M. Newmann, J. D. Robb, and J. R. Stahmann, "Lightning Protection Measures for Aircraft Fuel Systems, Phase II." Lightning and Transients Research Institute, FAA Technical Report ADS-18, May 1964.

10. Anon., "Lightning and Static Electricity Conference." Air Force Avionics Laboratory, Air Force Systems Command, Wright-Patterson Air Force Base, AFAL-TR-68-290, May 1969.

11. K. J. Lloyd, J. A. Plumer, and L. C. Walko, "Measurements and Analysis of Lightning-Induced Voltages in Aircraft Electrical Systems." General Electric Company, High Voltage Laboratory, HVL 69-161, March 1970. Will be published as NASA Contractor Report.

12. J. H. Hagenguth and J. G. Anderson, "Lightning to the Empire State Building - Part III." AIEE Trans., Vol. 71, Part III (Power Apparatus and Systems), pp. 641-649, August 1952.

13. K. B. McEachron, "Lightning to the Empire State Building." AIEE Trans., Vol. 60, pp. 885-890, 1941.

TABLE I. - INDUCED VOLTAGES AND CURRENT

[Circuit L.050, Position Light
Conductor 2L10E18 and Airframe.]

i_L Wave Form:	Slow wave form (36 × 82 μs)				Fast wave form (8.2 × 14 μs)			
Stroke location	Open circuit voltage, e_{oc}, V	Short circuit current, i_{sc}, A	Voltage across 1-ohm load, e_l, V	Current through 1-ohm load, i_l, A	Open circuit voltage, e_{oc}, V	Short circuit current, i_{sc}, A	Voltage across 1-ohm load, e_l, V	Current through 1-ohm load, i_l, A
1 Forward end of tip tank	40/20	9.0	6.0	6.0	96/48	15.0	12.0	11.0
4 Outboard leading edge	6/2.2	0.8	3/0.6	0.6	15/4	1.1	0.7	0.65
5 Trailing edge of aileron	15/3.8	1.3	1.0	1.0	30/12	4.0	3.0	3.0
7 Center of wing surface	10/2.4	0.8	0.8	0.7	20/2	1.5	1.2	1.2
10 Inboard leading edge	10/1.8	0.7	0.8	0.5	17/2.8	1.7	2.8/0.7	0.65

TABLE II. - CALCULATED EFFECTIVE WING RESISTANCES AND MUTUAL INDUCTANCES FOR VARIOUS TEST CONDITIONS

[Circuit L.050, Position Light Conductor 2L10E18 and Airframe.]

i_L Wave form:	Slow wave form (36 × 82 μs)		Fast wave form (8.2 × 14 μs)	
Stroke location	R_W, μΩ	M, nH	R_W, μΩ	M, nH
1 Forward end of tip tank	450.0	16.3	700.0	4.25
4 Outboard leading edge	57.5	0.032	70.0	0.5
5 Trailing edge of aileron	25.0	2.75	-100.0	1.55
7 Center of wing surface	45.0	1.68	-40.0	0.244
10 Inboard leading edge	40.0	0.022	60.0	0.31

TABLE III. - CALCULATED THEVENIN IMPEDANCE SERIES R AND L COMPONENTS FOR VARIOUS TEST CONDITIONS

[Circuit L.050, Position Light Conductor 2L10E18 and Airframe.]

Lightning current wave shape:	8.2 × 14 μs		36 × 82 μs	
Stroke location	R, Ω	L, μH	R, Ω	L, μH
1 Forward end of tip tank	1.98	11.2	----	-----
4 Outboard leading edge	3.33	0.39	2.65	-7.8
5 Trailing edge of aileron	1.23	8.0	2.3	36.2
7 Center of wing surface	----	-----	2.63	8.37
10 Inboard leading edge	3.09	5.7	2.29	9.56

TABLE IV. - INDUCED VOLTAGES AND CURRENTS

[Circuit F.0511, E-11 Autopilot Conductors F572K18 and F755E18.]

i_L Wave form:	Slow wave form (36 × 82 μs)				Fast wave form (8.2 × 14 μs)			
Stroke location	Open circuit voltage, e_{oc}, V	Short circuit current, i_{sc}, A	Voltage across 1-ohm load, e_l, V	Current through 1-ohm load, i_l, A	Open circuit voltage, e_{oc}, V	Short circuit current, i_{sc}, A	Voltage across 1-ohm load, e_l, V	Current through 1-ohm load, i_l, A
1 Forward end of tip tank	0.07	0.3	0.068	0.075	0.4	0.2	0.23/ 0.23	0.2
4 Outboard leading edge	27/0.1	0.25	0.2/ 0.12	0.1	3/0.48	0.5	0.26	0.2
5 Trailing edge of aileron	2/0.2	0.25	0.4/ 0.13	0.1	0.6	0.5	0.3	0.25
7 Center of wing surface	0.1	0.25	0.12	0.1	6/0.5	0.5	0.3	0.25
10 Inboard leading edge	0.1	0.25	0.04	0.04	1.5/ 0.2	0.1	0.1	0.1

TABLE V. - CALCULATED EFFECTIVE WING RESISTANCES AND MUTUAL INDUCTANCES FOR VARIOUS TEST CONDITIONS

[Circuit F.0511, E-11 Autopilot
Conductors F572K18 and F755E18.]

i_L Wave form:	Slow wave form (36 × 82 μs)		Fast wave form (8.2 × 14 μs)	
Stroke location	R_W, μΩ	M, nH	R_W, μΩ	M, nH
1 Forward end of tip tank	0.75	-0.0185	4.5	-0.0698
4 Outboard leading edge	0.50	-0.0684	2.0	-0.187
5 Trailing edge of aileron	1.25	-0.0392	8.25	-0.107
7 Center of wing surface	0.375	-0.0169	10.0	-0.117
10 Inboard leading edge	2.25	-0.043	1.75	-0.0227

TABLE VI. - MAXIMUM INDUCED VOLTAGES AND CURRENTS IN NEW WING CIRCUITS

[Series 1 - Measurements at leading edge on entire length of circuits. Trailing edge terminations connected to airframe.]

Conductor	Open circuit voltage, V		Short circuit current, A	
	Conductor-to-airframe	Conductor-to-conductor	Conductor-to-airframe	Conductor-to-conductor
Unshielded number 16 insulated conductor	1.5	----	0.8	---
RG 58A/U coaxial cable	1.2	----	1.6	---
Twisted pair of number 16 insulated conductors	1.5	0.16	1.0	0.1
Parallel pair of number 16 insulated conductors	5.0	1.6	5.0	0.8

TABLE VII. - MAXIMUM INDUCED VOLTAGES AND CURRENTS IN NEW WING CIRCUITS

[Series 2 - All circuits and shields connected to airframe at location between aileron and flap on trailing edge. Identical measurements on circuits terminating at leading and trailing edges.]

Conductor	Open circuit voltage, V				Short circuit current, A			
	Conductor-to-airframe		Conductor-to-conductor		Conductor-to-airframe		Conductor-to-conductor	
	Leading edge[a]	Trailing edge[b]	Leading edge	Trailing edge	Leading edge	Trailing edge	Leading edge	Trailing edge
Unshielded number 16 insulated conductor	2.0	0.4	----	----	1.6	1.3	---	---
RG 58A/U coaxial cable	2.1	0.4	----	----	2.2	0.4	---	---
Twisted pair of number 16 insulated conductors	1.0	0.5	0.22	0.04	1.4	0.9	0.1	0.1
Parallel pair of number 16 insulated conductors	6.0	1.0	2.3	0.1	6.0	2.0	1.3	0.1

[a]Circuits terminating at leading edge are 38 feet long.
[b]Circuits terminating at trailing edge are 12 feet long.

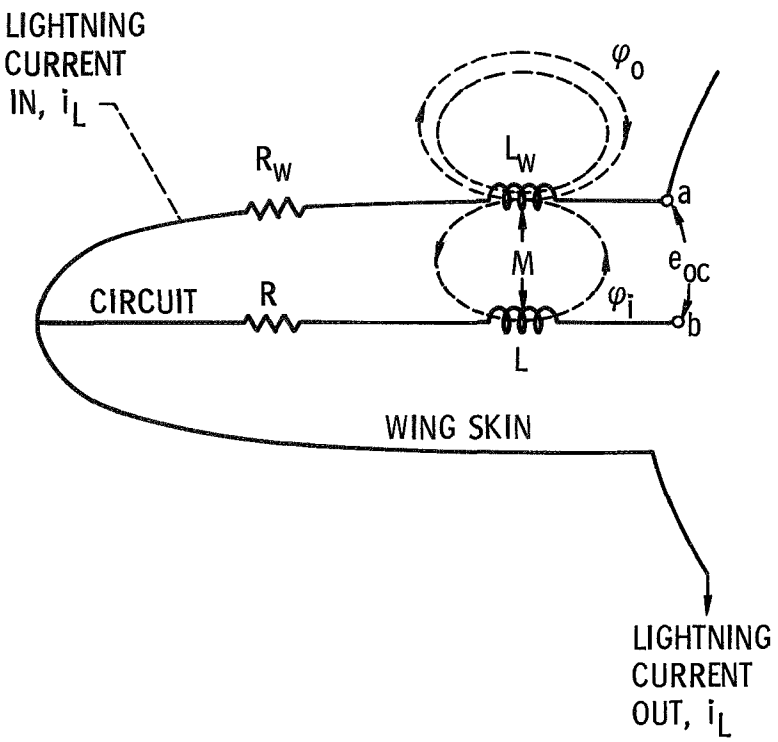

Figure 1. - Circuit representation of aircraft wing-electrical circuit combination.

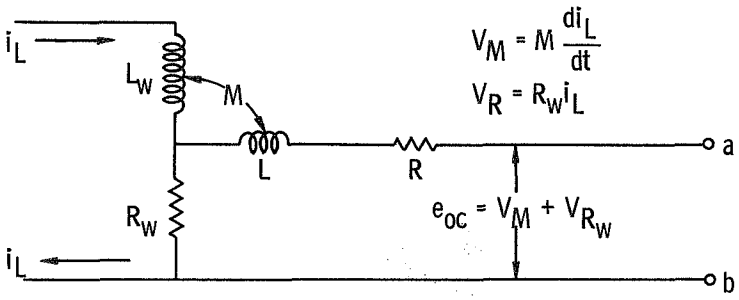

Figure 2. - Circuit representation of wing structure and electrical circuit.

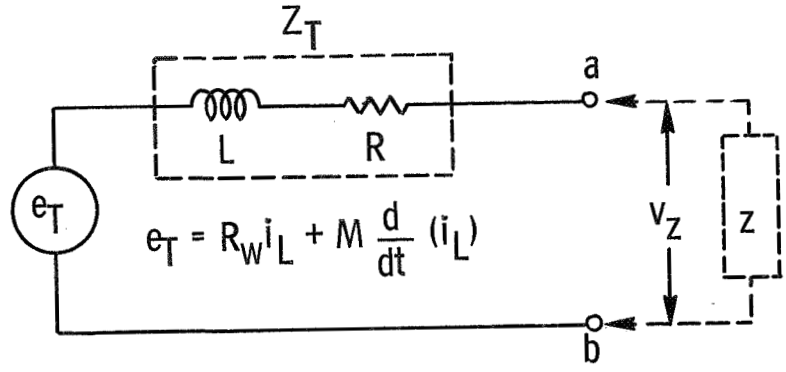

Figure 3. - Thevenin equivalent circuit.

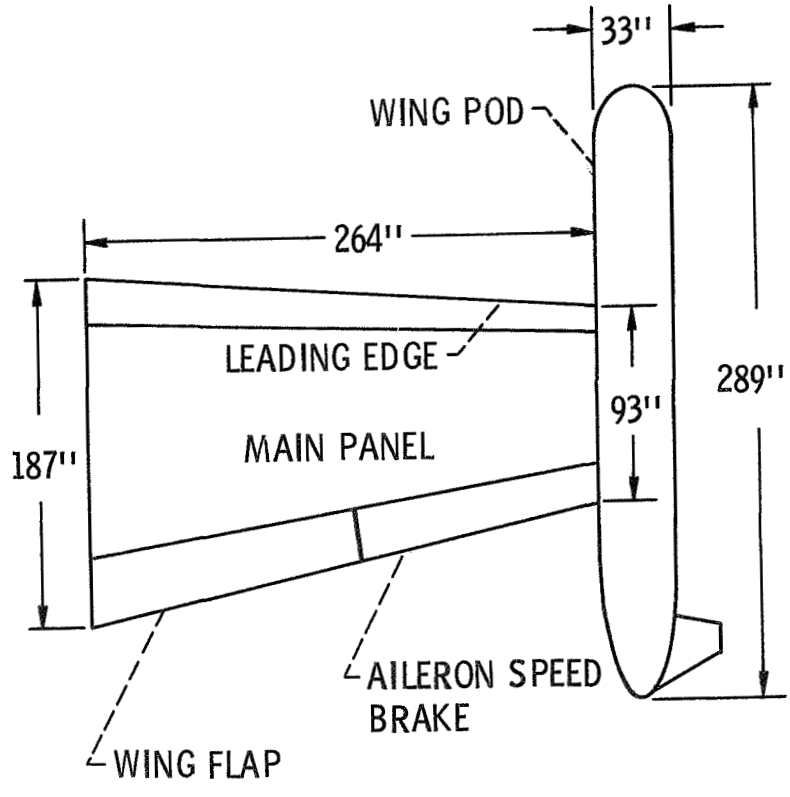

Figure 4. - Schematic plan view of wing.

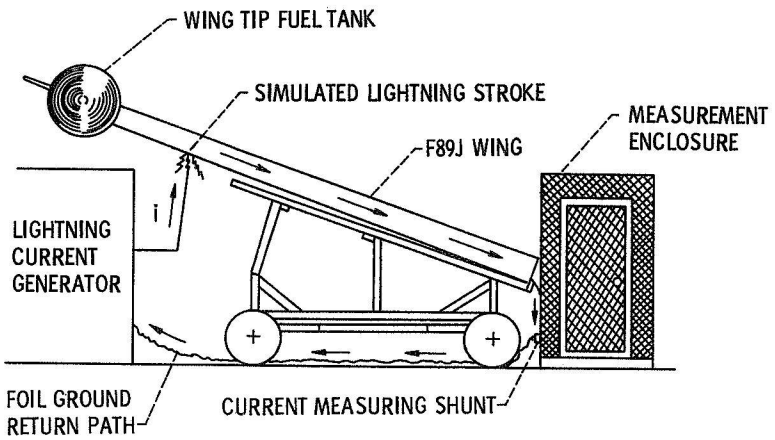

Figure 5. - F89J wing test setup.

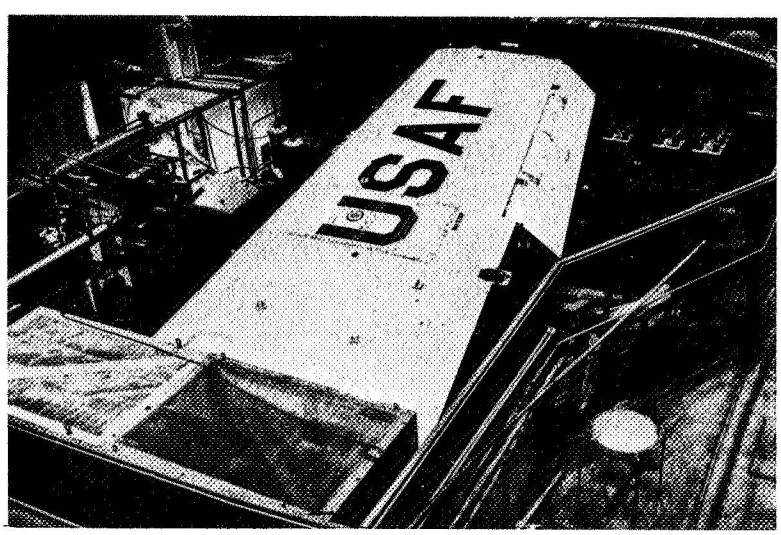

Figure 6. - F89J right wing shown positioned for test in high voltage laboratory test bay. Lightning current generator is beneath tip tank.

T_1 - FRONT TIME
T_2 - TIME TO HALF VALUE ON THE TAIL

THE WAVE SHAPE IS DESCRIBED BY THE NOTATION: $(T_1 \times T_2)$

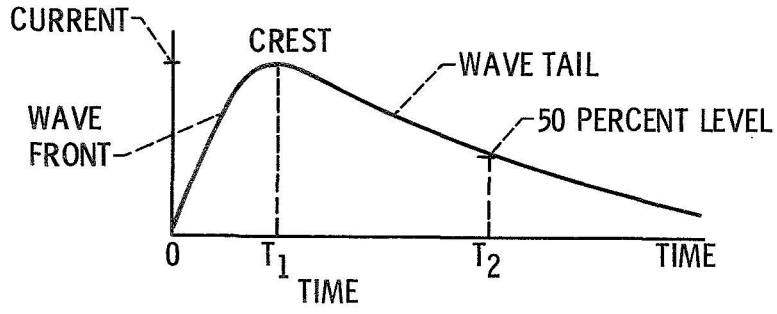

Figure 7. - Simulate lightning wave shape notation.

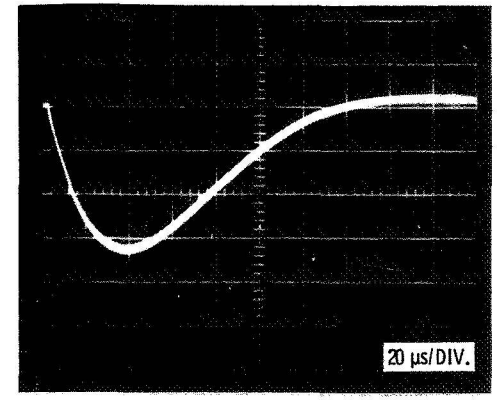

(A) "SLOW WAVE SHAPE" 36 x 82 μs.

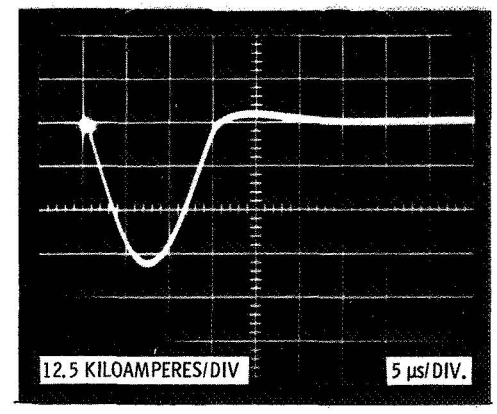

(B) "FAST WAVE SHAPE" 8.2 x 14 μs.

Figure 8. - Simulated lightning current wave shapes (40 kiloampere strokes, applied for induced effects measurements).

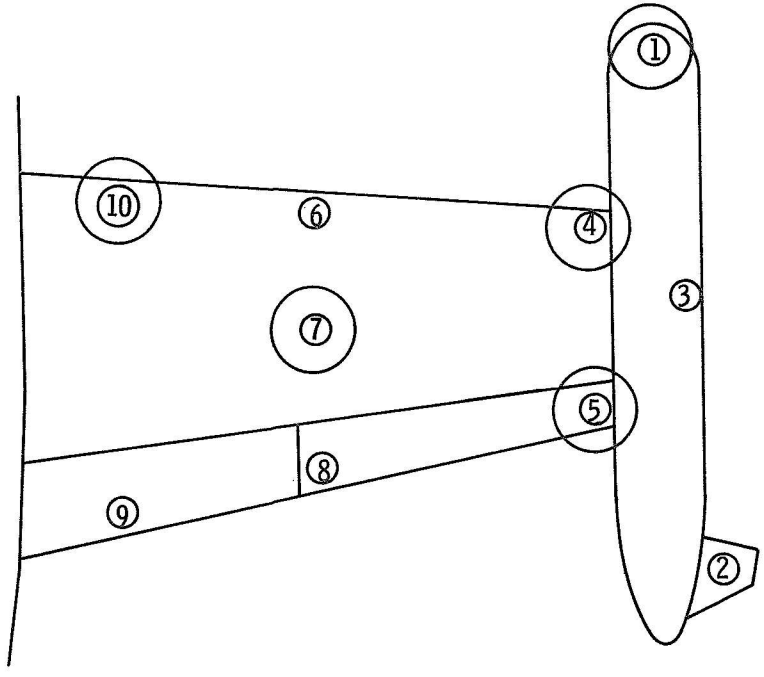

Figure 9. - Simulated lightning stroke locations. Large circled numbers indicate locations selected for extensive testing.

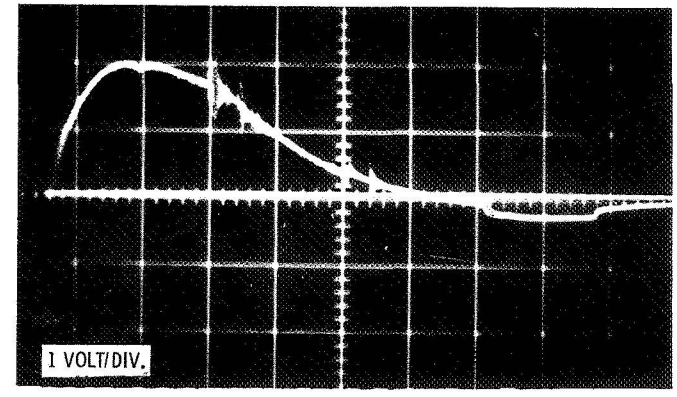

(A) OPEN CIRCUIT INDUCED VOLTAGE.

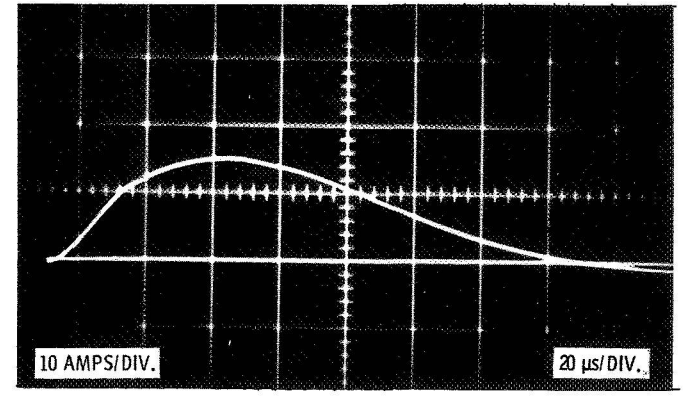

(B) SHORT CIRCUIT CURRENT.

Figure 10. - Open circuit induced voltage and short circuit current. 40 kiloampere 36 x 82 μs lightning stroke to location 1.

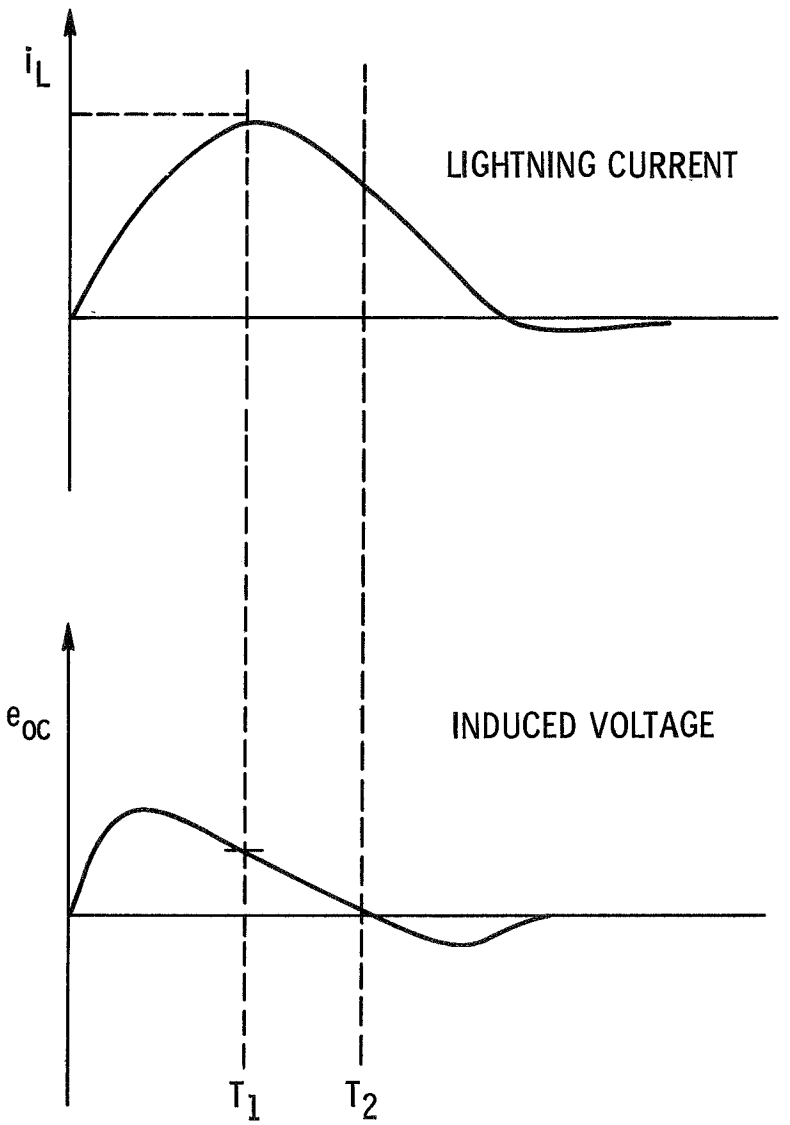

Figure 11. - Typical lightning current and induced voltage wave forms.

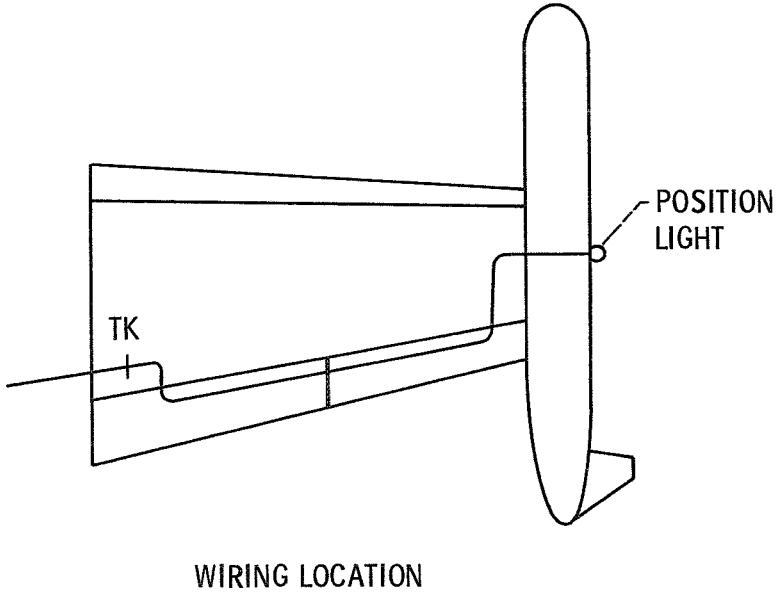

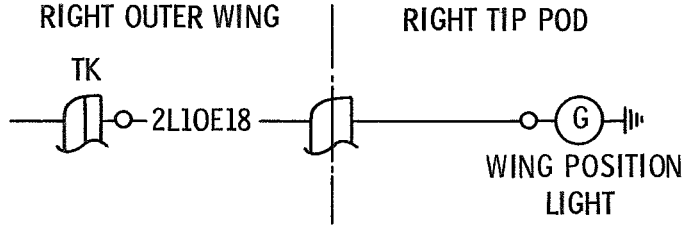

Figure 12. - Circuit 1.050 position lights wiring schematic and location F89J right wing and tip fuel tank.

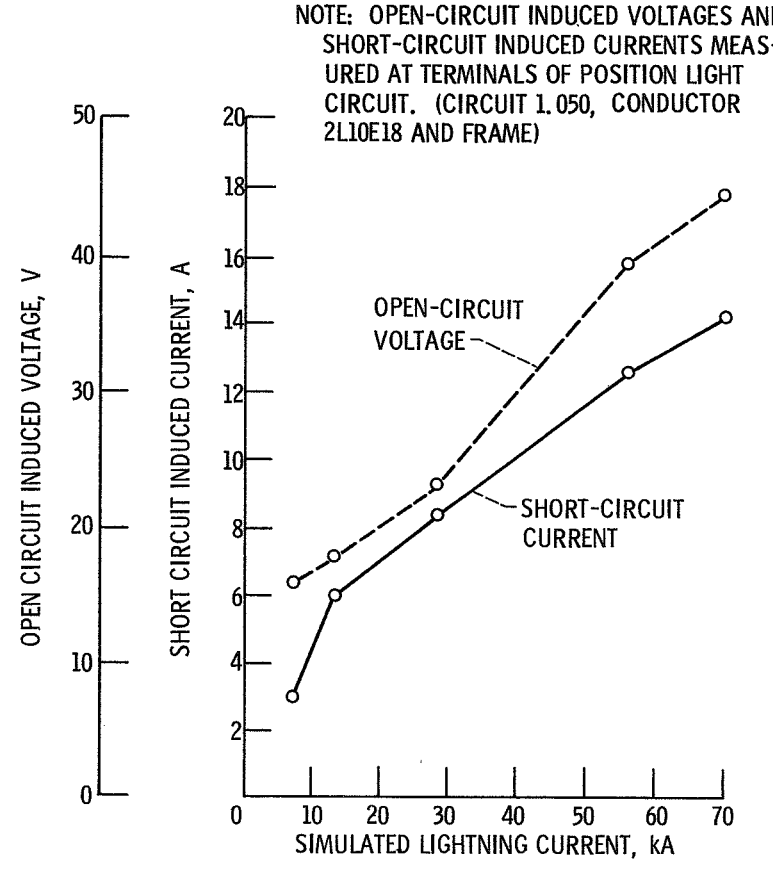

Figure 13. - Amplitude of induced effects versus amplitude of simulated 12 x 24 μs lightning current discharged to location number 1 (forward end of wing tip fuel tank).

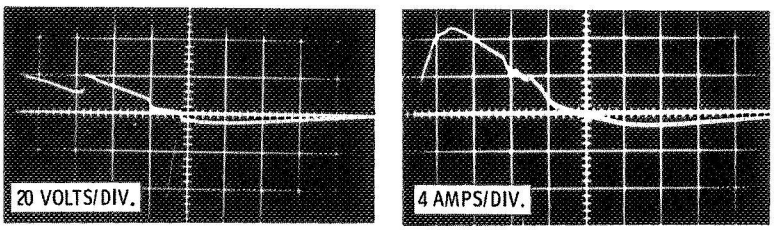

(A) STROKE LOCATION NO. 1, FORWARD END OF WING TIP FUEL TANK.

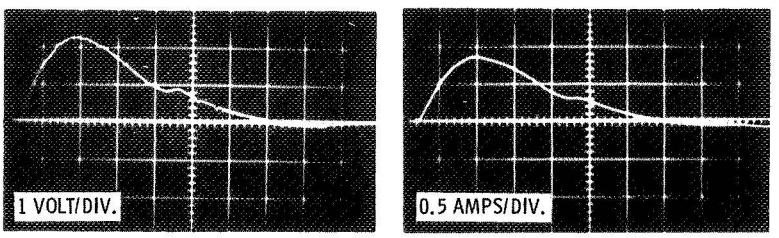

(B) STROKE LOCATION NO. 4, OUTBOARD END OF LEADING EDGE.

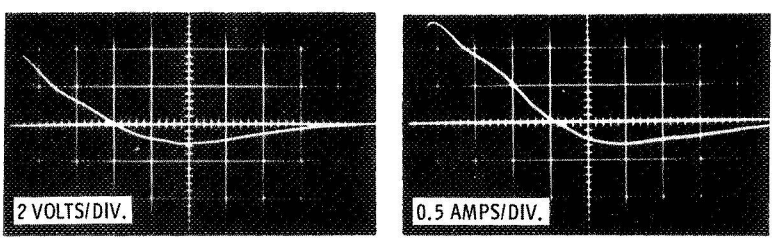

(C) STROKE LOCATION NO. 5, OUTBOARD END OF AILERON.

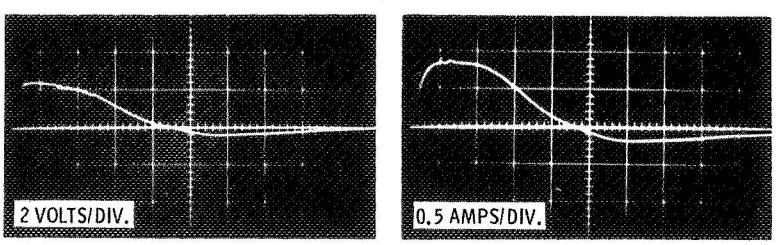

(D) STROKE LOCATION NO. 7, BOTTOM CENTER OF WING.

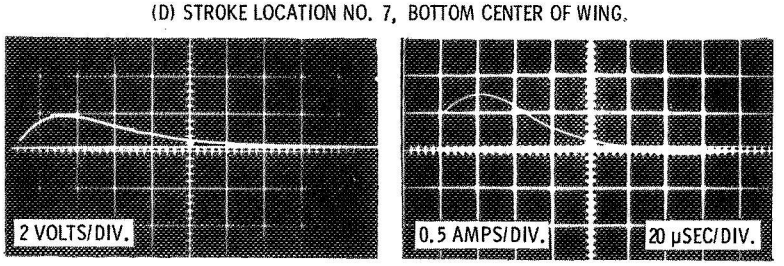

OPEN CIRCUIT VOLTAGE SHORT CIRCUIT CURRENT

(E) STROKE LOCATION NO. 10, INBOARD LEADING EDGE OF WING.

Figure 14. - Open circuit voltages and short circuit currents measured on terminals of circuit L.050 (position light), conductor 2L10E18 to airframe. (36 x 82 µsec, 40 kiloampere simulated lightning current.)

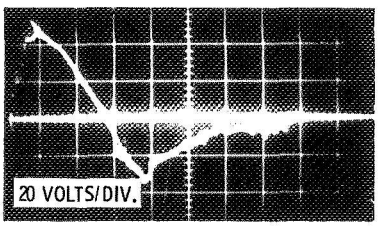

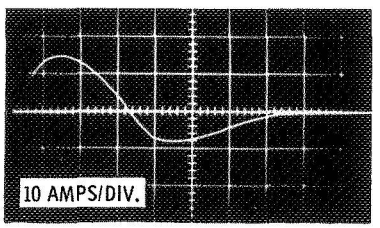

(A) STROKE LOCATION NO. 1, FORWARD END OF WING TIP FUEL TANK.

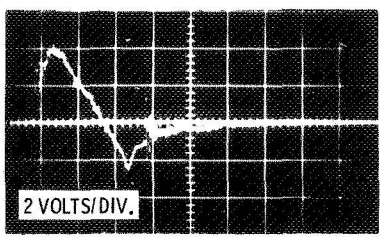

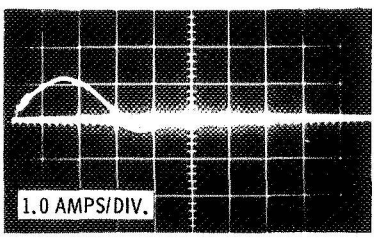

(B) STROKE LOCATION NO. 4, OUTBOARD END OF LEADING EDGE.

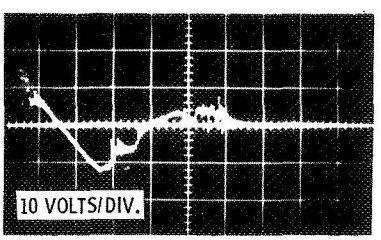

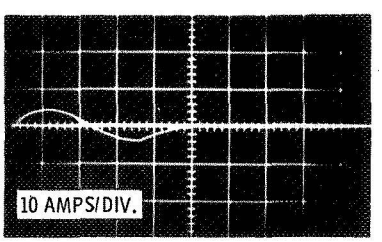

(C) STROKE LOCATION NO. 5, OUTBOARD END OF AILERON.

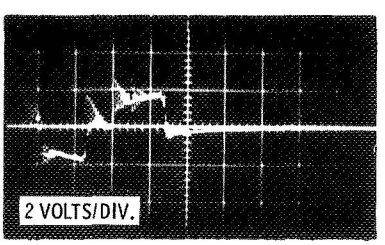

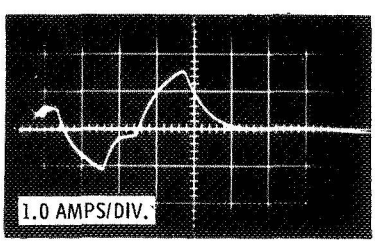

(D) STROKE LOCATION NO. 7, BOTTOM CENTER OF WING.

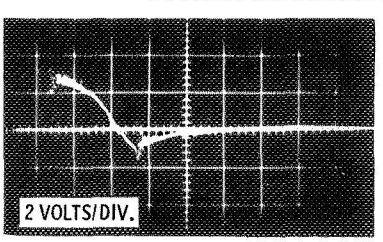

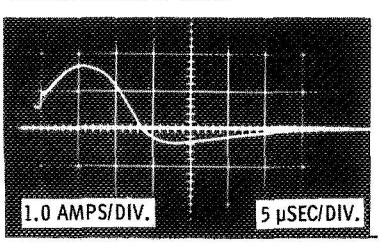

OPEN CIRCUIT VOLTAGE SHORT CIRCUIT CURRENT

(E) STROKE LOCATION NO. 10, INBOARD LEADING EDGE OF WING.

Figure 15. - Open circuit voltages and short circuit current measured on terminals of circuit L.050 (position light), conductor 2L10E18 to airframe. (8.2 x 14 µsec, 40 kiloampere simulated lightning current.)

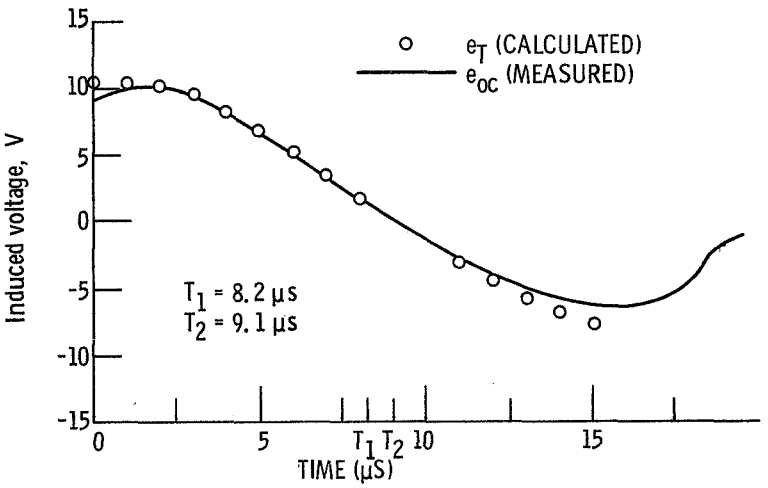

Figure 16. - Comparison of measured e_{oc} and calculated e_T induced voltage wave shapes, resulting from 40 kiloampere 8.2 x 14 μs stroke to location 1.

E-5991

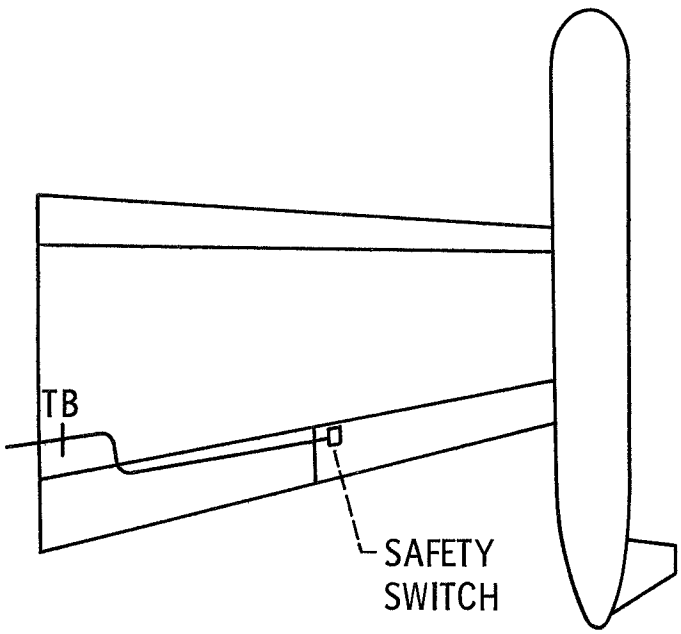

WIRING LOCATION

RIGHT OUTERWING

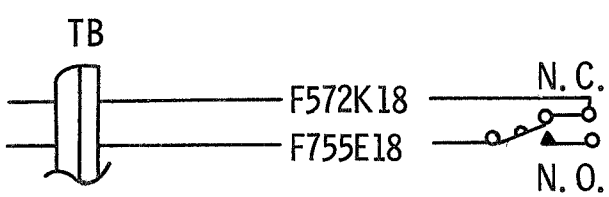

RIGHT ROCKET
SAFETY SWITCH

Figure 17. - Circuit F.0511 E-11 autopilot flap position monitoring switch wiring schematic and location F89J right wing and tip fuel tank.

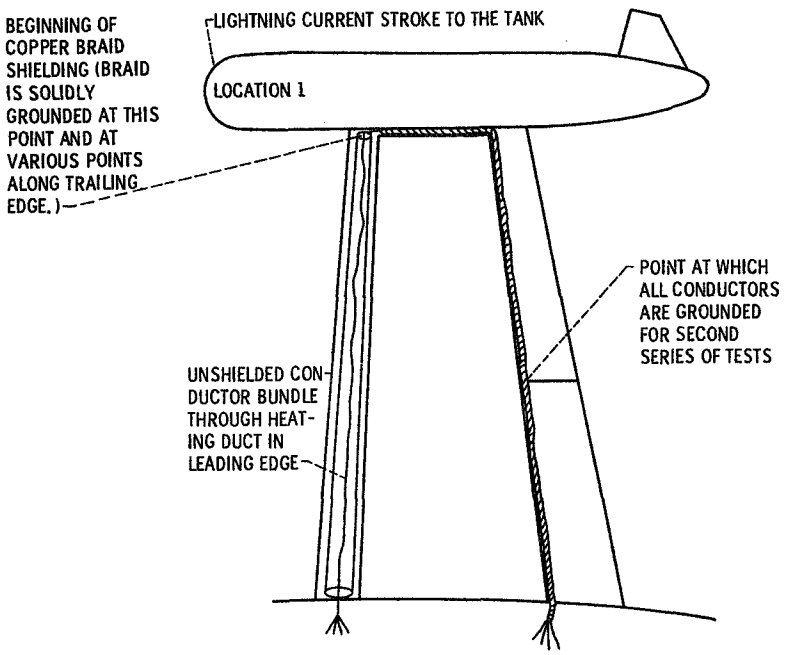

Figure 18. - F-89 Wing showing additional circuits placed in the wing for test.

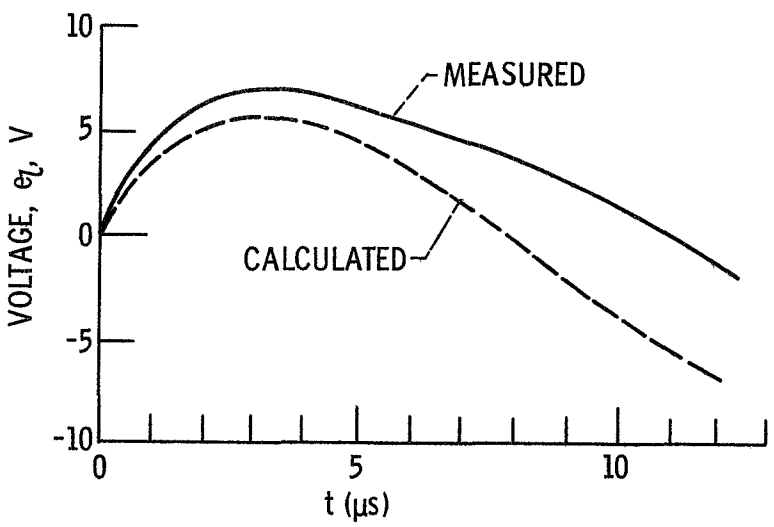

Figure 19. - Verification of Thevenin circuit calculation of voltage across 1-ohm resistive load. 40 Kiloampere, 8.2 x 14 μs lightning current to location 1.